Instability of Rotationally Tuned Dipolar Bose-Einstein Condensates

S. B. Prasad,[1] T. Bland,[2] B. C. Mulkerin,[3] N. G. Parker,[1,2] and A. M. Martin[1]
[1]School of Physics, University of Melbourne, Melbourne 3010, Australia
[2]Joint Quantum Centre Durham-Newcastle, School of Mathematics, Statistics and Physics, Newcastle University, Newcastle upon Tyne, NE1 7RU, United Kingdom
[3]Centre for Quantum and Optical Science, Swinburne University of Technology, Melbourne 3122, Australia

(Received 21 October 2018; revised manuscript received 4 December 2018; published 6 February 2019)

The possibility of effectively inverting the sign of the dipole-dipole interaction, by fast rotation of the dipole polarization, is examined within a harmonically trapped dipolar Bose-Einstein condensate. Our analysis is based on the stationary states in the Thomas-Fermi limit, in the corotating frame, as well as direct numerical simulations in the Thomas-Fermi regime, explicitly accounting for the rotating polarization. The condensate is found to be inherently unstable due to the dynamical instability of collective modes. This ultimately prevents the realization of robust and long-lived rotationally tuned states. Our findings have major implications for experimentally accessing this regime.

DOI: 10.1103/PhysRevLett.122.050401

Dipolar Bose-Einstein condensates (BECs) have proved to be a unique, highly controllable platform for studying the interplay of quantum many-body physics and magnetic interactions [1–6]. Compared to conventional condensates, in which the atoms undergo short-range, contact-like, isotropic interparticle interactions, a dipolar BEC also enjoys a long-range anisotropic dipole-dipole interaction (DDI) [7–11]. While the first dipolar BECs were realized in a gas of ^{52}Cr [1,2], atoms with larger magnetic dipole moments such as ^{164}Dy [4,6] and ^{168}Er [5] have now been cooled to form strongly dipolar BECs. This has led to the observation of magnetostriction [12], dipole mediated stability [13,14], anisotropic superfluidity [15], dipolar gap solitons in 2D free space [16], the roton mode [17–19], and the discovery of self-bound dipolar droplets [6,20–22].

The net interaction potential, combining the contact interactions and DDI, is pivotal to both the stability of the gas and to realize regimes of novel physics. To date, experimentalists have controlled this potential by exploiting Feshbach resonances to tune the contact interaction, thereby allowing for DDI-dominated regimes [13,14]. Furthermore it has been suggested that the magnitude and sign of the DDI can be tuned via rotation of the dipole moments [23]. Consider a BEC of bosons with magnetic dipole moment μ_d, polarized uniformly along an axis $\hat{\mathbf{e}}(t)$, such that the DDI is

$$U_{\rm dd}(\mathbf{r},t)=\frac{C_{\rm dd}}{4\pi}\frac{1-3[\hat{\mathbf{e}}(t)\mathbf{r}]^2}{|\mathbf{r}|^3}, \tag{1}$$

where $C_{\rm dd}=\mu_0\mu_d^2$ and μ_0 is the vacuum permeability. If $\hat{\mathbf{e}}(t)$ rotates about the z axis at a tilt angle φ, the time averaged DDI over one rotation cycle is [23]

$$\langle\!\langle U_{\rm dd}(\mathbf{r})\rangle\!\rangle=\frac{C_{\rm dd}}{4\pi}\left(\frac{3\cos^2\varphi-1}{2}\right)\left(\frac{1-3(\hat{z}\cdot\mathbf{r})^2}{|\mathbf{r}|^3}\right). \tag{2}$$

Thus, in the rapid-rotation limit, the tilt angle φ may be used to tune the effective strength of the DDI and in particular, when $\cos^2\varphi>1/3$, the effective DDI strength becomes negative, corresponding to an unusual "antidipolar" regime in which side-by-side alignment of the dipole moments is energetically preferred to head-to-tail alignments. Subsequent theoretical studies of dipolar BECs in this regime, which invoked the rotational tuning mechanism by setting $C_{\rm dd}<0$, led to predictions of novel physics such as molecular bound states in dark solitons [24], multidimensional dark [25] and bright [26,27] solitons, stratified turbulence [28], and the roton instability of vortex lines [29]. In this direction, a recent experimental study of rotational tuning by Tang *et al.* [30] has reported a realization of the antidipolar regime.

In this Letter we revisit rotational tuning of a dipolar BEC, in a cylindrically symmetric harmonic trap of the form $V_{\rm T}(\mathbf{r})=\frac{1}{2}m\omega_\perp^2(x^2+y^2+\gamma^2z^2)$, and model polarization rotational angular frequencies, Ω, greater than $\omega_\perp$. This rotation is seen to result in an asymmetry of the condensate about $\hat{z}$ that is not evident if the DDI due to a rotating polarization is directly replaced by its time-averaged counterpart. This asymmetry results in a dynamical instability, similar to those predicted [31–33] and observed [34,35] for nondipolar condensates in rotating ellipsoidal traps, that prevents the formation of a dynamically stable rotationally tuned state. This is elucidated via two distinct approaches, one being based on a semianalytical treatment in the *Thomas-Fermi* (TF) limit, and the other being time-dependent numerical simulations.

These results raise major questions over the pursuit of rotational tuning of dipolar BECs.

As the maximally antidipolar regime occurs for $\varphi = \pi/2$, we consider the polarizing field $\hat{\mathbf{e}}$ to be rotating in the x-y plane at angular frequency Ω, and work in a reference frame corotating with $\mathbf{e}$ such that we may fix $\hat{\mathbf{e}} = \hat{x}$ in this frame. Then, the dipolar condensate order parameter $\psi(\mathbf{r}, t)$ [36] for bosons of mass m can be modeled by the dipolar Gross-Pitaevskii equation (DGPE),

$$i\hbar\frac{\partial\psi}{\partial t} = \left[-\frac{\hbar^2\nabla^2}{2m} + V_{\mathrm{T}} + V_{\mathrm{int}} + i\hbar\Omega\left(x\frac{\partial}{\partial y} - y\frac{\partial}{\partial x}\right)\right]\psi. \tag{3}$$

Assuming that the rotation frequency is slow enough that the dipole moments remain aligned along $\hat{\mathbf{e}}$ at all times, the interaction potential V_{int} is specified by [37]

$$V_{\mathrm{int}}(\mathbf{r}, t) = g|\psi(\mathbf{r}, t)|^2 + \int d\mathbf{r}' U_{\mathrm{dd}}(\mathbf{r} - \mathbf{r}')|\psi(\mathbf{r}', t)|^2, \tag{4}$$

where $g = 4\pi\hbar^2 a_s/m$ and a_s is the bosonic s-wave scattering length. The DDI strength may be related to a_s through a dimensionless ratio $\epsilon_{\mathrm{dd}} = C_{\mathrm{dd}}/(3g)$.

Previous studies of rotationally tuned dipolar BECs have involved setting $\Omega = 0$ and replacing U_{dd} with $\langle\langle U_{\mathrm{dd}}\rangle\rangle$ in Eq. (4). To test the validity of this procedure, we solve for the stationary solutions of Eq. (3), which obey $i\hbar\partial_t\psi = \mu\psi$, with μ being the condensate's chemical potential. We reexpress the order parameter as $\psi = \sqrt{n}\exp(iS)$, where S is the condensate phase and n, the condensate density, is normalized to the condensate number N via $\int d^3 r n(\mathbf{r}) = N$. In the TF limit, obtained by neglecting the zero-point kinetic energy of the condensate [38], the stationary solutions are of the form

$$n_{\mathrm{TF}}(\mathbf{r}) = n_0\left(1 - \frac{x^2}{\kappa_x^2 R_z^2} - \frac{y^2}{\kappa_y^2 R_z^2} - \frac{z^2}{R_z^2}\right). \tag{5}$$

$$S_{\mathrm{TF}}(\mathbf{r}, t) = \alpha xy - \mu t/\hbar, \tag{6}$$

Here $n_0 = 15N/(8\pi\kappa_x\kappa_y R_z^3)$ is the peak density, R_i is the TF radius of the dipolar BEC along the i axis, and $\kappa_x = R_x/R_z$ and $\kappa_y = R_y/R_z$ are the condensate aspect ratios, with respect to $\hat{z}$, along $\hat{x}$ and $\hat{y}$, respectively.

The TF stationary solutions are uniquely determined by a set of consistency relations, whose derivation is presented in the Supplemental Material [39]. For a given choice of $\{\gamma, \epsilon_{\mathrm{dd}}, \Omega, \omega_\perp\}$, the consistency relations are given by:

$$\kappa_x^2 = \frac{1}{\zeta}\left(\frac{\omega_\perp\gamma}{\tilde{\omega}_x}\right)^2\left[1 + \epsilon_{\mathrm{dd}}\left(\frac{9}{2}\kappa_x^3\kappa_y\beta_{200} - 1\right)\right], \tag{7}$$

$$\kappa_y^2 = \frac{1}{\zeta}\left(\frac{\omega_\perp\gamma}{\tilde{\omega}_y}\right)^2\left[1 + \epsilon_{\mathrm{dd}}\left(\frac{3}{2}\kappa_y^3\kappa_x\beta_{110} - 1\right)\right], \tag{8}$$

$$0 = (\alpha + \Omega)\left[\tilde{\omega}_x^2 - \frac{9}{2}\epsilon_{\mathrm{dd}}\frac{\omega_\perp^2\kappa_x\kappa_y\gamma^2}{\zeta}\beta_{200}\right] + (\alpha - \Omega)\left[\tilde{\omega}_y^2 - \frac{3}{2}\epsilon_{\mathrm{dd}}\frac{\omega_\perp^2\kappa_x\kappa_y\gamma^2}{\zeta}\beta_{110}\right]. \tag{9}$$

Here, α, $\tilde{\omega}_x$, $\tilde{\omega}_y$, β_{ijk}, and ζ are defined by the following:

$$\alpha = \frac{\kappa_x^2 - \kappa_y^2}{\kappa_x^2 + \kappa_y^2}\Omega, \tag{10}$$

$$\tilde{\omega}_x^2 = \omega_\perp^2 + \alpha^2 - 2\alpha\Omega, \tilde{\omega}_y^2 = \omega_\perp^2 + \alpha^2 + 2\alpha\Omega, \tag{11}$$

$$\beta_{ijk} = \int_0^\infty (s + \kappa_x^2)^{-i-\frac{1}{2}}(s + \kappa_y^2)^{-j-\frac{1}{2}}(s + 1)^{-k-\frac{1}{2}}ds, \tag{12}$$

$$\zeta = 1 + \epsilon_{\mathrm{dd}}\left(\frac{3}{2}\kappa_x\kappa_y\beta_{101} - 1\right). \tag{13}$$

Equation (10) encapsulates the in-plane anisotropy of the stationary TF density as a function of Ω, with a positive (negative) α implying that the condensate density is elongated along $\hat{x}$ ($\hat{y}$). Figure 1 shows how α varies with Ω for [(a) and (b)] various values of ϵ_{dd} while fixing γ, and for [(c) and (d)] various values of γ while fixing ϵ_{dd}. If $\epsilon_{\mathrm{dd}} = 0$, $\alpha = 0$ is a valid solution for all Ω. A bifurcation occurs at $\Omega = \Omega_b$, with the addition of two new branches, symmetric about the Ω axis, that exist only for $\Omega_b \leq \Omega < \omega_\perp$. The symmetry about the Ω axis is broken when $\epsilon_{\mathrm{dd}} > 0$. Instead, we have $\alpha > 0$ when $0 < \Omega < \Omega_b$, and this branch persists for $\Omega_b \leq \Omega < \omega_\perp$. The bifurcation is now in the form of two additional $\alpha < 0$ solutions for $\Omega \geq \Omega_b$, which are simply connected to each other at $\Omega = \Omega_b$. The two branches with the highest $|\alpha(\Omega)|$ terminate at $\Omega = \omega_\perp$. This is characteristic of the TF limit in a rotating frame, with similar bifurcations occurring in a BEC rotating about the z

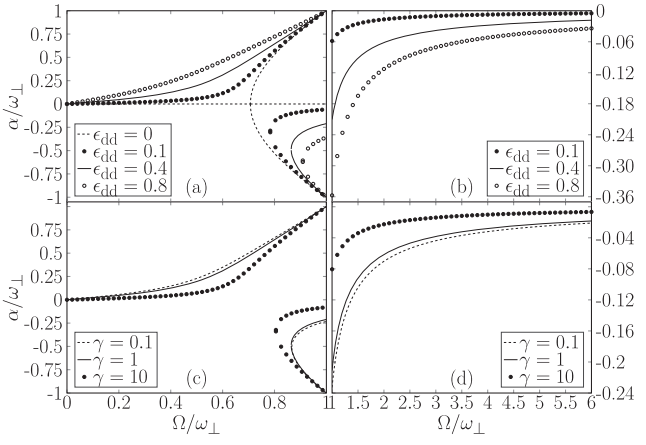

FIG. 1. Stationary solutions, as characterized by α, as a function of Ω: (a) and (b) $\gamma = 1$ and various ϵ_{dd}; (c) and (d) $\epsilon_{\mathrm{dd}} = 0.4$ and various γ. In (b), the $\gamma = 1$, $\epsilon_{\mathrm{dd}} = 0$ branch has $\alpha = 0$.

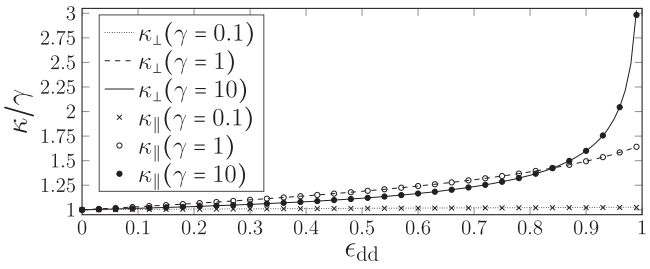

FIG. 2. Comparison of the solutions for the rapid-rotating dipoles and time-averaged DDI formalisms. Shown is $\kappa_\perp$ (lines) evaluated at $\Omega = 50\omega_\perp$ and $\kappa_\parallel$ (markers), with $\epsilon_{dd} \to -\epsilon_{dd}/2$, as a function of ϵ_{dd} and for various trap aspect ratios.

axis with a planar trapping ellipticity, with or without z-polarized dipoles [31,40,48,49]. This has been attributed to the $L_z = 2$ quadrupole mode being energetically unstable for $\Omega > \Omega_b$, resulting in $\Omega_b(\epsilon_{dd} = 0) = \omega_\perp/\sqrt{2}$ as demonstrated in Fig. 1(a) [31,50].

It is evident that these rotating-frame solutions tend towards cylindrical symmetry ($\alpha = 0$) as $\Omega \to \infty$. We proceed to test whether they agree with the nonrotating TF stationary solutions found by utilizing the time-averaged DDI. The latter are exactly symmetric about $\hat{z}$ and possess an aspect ratio $\kappa_\parallel \equiv \kappa_x = \kappa_y$ specified via [41,42]

$$3\epsilon_{dd}\kappa_\parallel^2\left[\left(1+\frac{\gamma^2}{2}\right)\frac{f(\kappa_\parallel)}{1-\kappa^2}-1\right] = (\epsilon_{dd}+2)(\gamma^2-\kappa_\parallel^2), \quad (14)$$

$$f(\kappa_\parallel) = \frac{1+2\kappa_\parallel^2}{1-\kappa_\parallel^2} - \frac{3\kappa_\parallel^2 \operatorname{arctanh}\sqrt{1-\kappa_\parallel^2}}{(1-\kappa_\parallel^2)^{3/2}}. \quad (15)$$

We compare this with the true time-averaged condensate density by transforming Eq. (5) to the laboratory coordinates and time-averaging over one rotation cycle, yielding the time-averaged aspect ratio $\kappa_\perp = \sqrt{2}(\kappa_x^{-2} + \kappa_y^{-2})^{-1/2}$.

Figure 2 compares $\kappa_\perp$ and $\kappa_\parallel$ as a function of ϵ_{dd}, with a range of trapping aspect ratios, γ, being considered and with $\kappa_\perp$ evaluated at a suitably high rotation frequency ($\Omega = 50\omega_\perp$). An almost perfect agreement between the two methodologies is evident. Note that when $\gamma = 1$, the condensate is flattened with respect to the z axis, consistent with an effective side-by-side orientation of z-polarized dipole moments.

To verify the stationary solutions, Eqs. (7)–(9), we numerically solve the 3D DGPE for a dipolar BEC of $N = 10^5$ bosons; N is chosen to be sufficiently large for a meaningful comparison with the TF analysis [38]. With Ω and γ fixed throughout, our initial condition is the stationary state for $\epsilon_{dd} = 0$ obtained by imaginary time propagation of the DGPE [43]. In time, ϵ_{dd} is slowly ramped up (at a rate $d\epsilon_{dd}/dt = 10^{-3}\omega_\perp$), such that the condensate can slowly traverse the corresponding stationary solutions to high adiabaticity. Further details

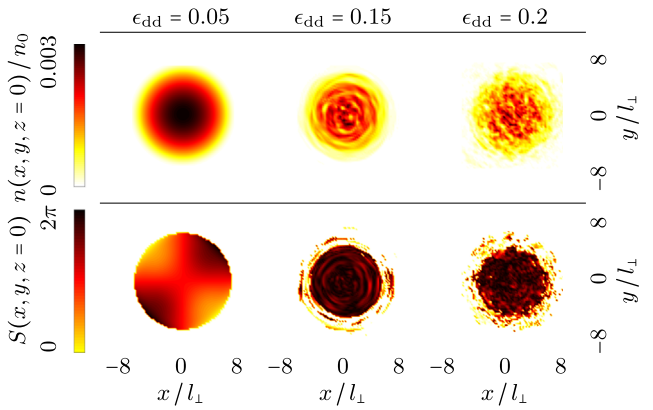

FIG. 3. Simulation of a dipolar BEC during an adiabatic ramp-up of ϵ_{dd}, with $N = 10^5$, $\gamma = 1$, and $\Omega = 3\omega_\perp$: cross sections at $z = 0$ of density (first row) and phase (second row) at $t = 50\omega_\perp^{-1}$ (first column), $t = 150\omega_\perp^{-1}$ (second column), and $t = 200\omega_\perp^{-1}$ (third column), scaled by $l_\perp = \sqrt{\hbar/(m\omega_\perp)}$. The density is normalized to $n_0 = N/l_\perp^3$.

regarding the simulation are provided in the Supplemental Material [39].

Figure 3 depicts the density and phase, during a simulation with fixed $\Omega = 3\omega_\perp$ and $\gamma = 1$, as cross sections at $z = 0$ (taken at times when $\epsilon_{dd} = 0.05$, 0.15, and 0.20). For low ϵ_{dd}, the condensate is consistent with the TF stationary solution: the density is smooth and approximates the paraboloid profile of Eq. (5), while the phase approximates the quadrupolar flow of Eq. (6). However, for higher ϵ_{dd}, the density and phase profiles deviate considerably from this form, first visible through a rippling of the density being evident ($\epsilon_{dd} = 0.15$), which later evolves towards a fragmented state ($\epsilon_{dd} = 0.2$). Figure 4 tracks this departure from the TF solution by comparing α as determined from the simulation with that found from Eqs. (7)–(9). While the agreement is excellent at low ϵ_{dd}, i.e., early time, the numerical value begins to fluctuate at $\epsilon_{dd} \approx 0.075$. The amplitude of this fluctuation grows with

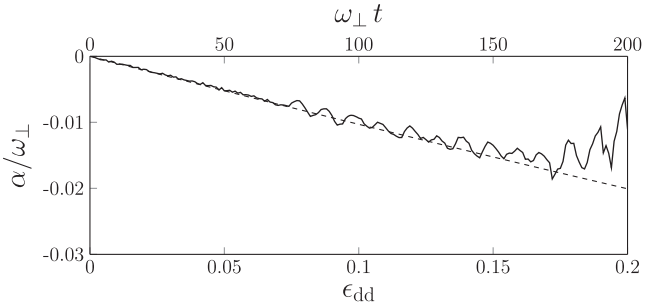

FIG. 4. Comparison between the numerical simulation and the TF solutions: α as a function of ϵ_{dd} at $\Omega = 3\omega_\perp$ and $\gamma = 1$, determined via Eqs. (7)–(9) (dashed line) and numerical simulation for $N = 10^5$ (solid line).

time, with the numerical solution diverging from the semianalytical one entirely when $\epsilon_{\rm dd} \approx 0.17$.

The deviation of the numerically determined α from the semianalytical prediction hints at the unstable growth of collective modes of the condensate [51]. This motivates us to return to the TF solutions to study their response to perturbations by means of linearized perturbation analysis [32,40,52]. We proceed by writing the time-dependent density and phase as fluctuations about the respective stationary state values:

$$n(\mathbf{r},t) = n_{\rm TF}(\mathbf{r}) + \delta n(\mathbf{r},t); \tag{16}$$

$$S(\mathbf{r},t) = S_{\rm TF}(\mathbf{r},t) + \delta S(\mathbf{r},t). \tag{17}$$

These are substituted into Eq. (3), with terms quadratic (or higher) in the fluctuations being discarded. This results in an eigenvalue problem of the form [32,33,40,49]

$$\frac{\partial}{\partial t}\begin{pmatrix}\delta S\\ \delta n\end{pmatrix} = \mathcal{L}\begin{pmatrix}\delta S\\ \delta n\end{pmatrix}, \tag{18}$$

where the explicit expression for the operator $\mathcal{L}$ is specified in the Supplemental Material [39]. The solutions of Eq. (18) are collective oscillations, and their respective eigenvalues obey

$$\begin{pmatrix}\delta S(\mathbf{r},t)\\ \delta n(\mathbf{r},t)\end{pmatrix} \equiv e^{\lambda t}\begin{pmatrix}\delta S(\mathbf{r})\\ \delta n(\mathbf{r})\end{pmatrix} : \mathcal{L}\begin{pmatrix}\delta S(\mathbf{r})\\ \delta n(\mathbf{r})\end{pmatrix} = \lambda\begin{pmatrix}\delta S(\mathbf{r})\\ \delta n(\mathbf{r})\end{pmatrix}. \tag{19}$$

Examining the spectra of Eq. (19) allows for a qualitative understanding of the stability of the condensate with respect to collective modes. If a mode, indexed by i, features $\mathrm{Re}(\lambda_i) > 0$, its amplitude grows exponentially and ultimately overwhelms the TF stationary solution. Thus, a stationary state is dynamically stable only if the real components of its entire spectrum is negative or zero.

Equation (19) may be diagonalized numerically over $\mathbb{R}^3$ by utilizing a polynomial basis $\{x^p y^q z^r\}$ for $\delta S(\mathbf{r})$ and $\delta n(\mathbf{r})$ [32,40]. Fluctuations of order $p+q+r = 0, 1, 2, \ldots$, represent monopolar, dipolar, and quadrupolar modes, respectively, and so on [44]; a rich variety of collective modes, including breathing and scissors modes, have been observed in several dipolar BEC experiments [51]. Due to the inability of a numerical diagonalization scheme to explore the infinite dimensional space of polynomials, it is necessary to impose a truncation of the form $p+q+r \leq N_{\rm max}$. However, we note that reducing the degree of the Hilbert space truncation, i.e., increasing $N_{\rm max}$, does not modify any eigenvalues corresponding to modes with an order less than $N_{\rm max}$, but merely increases the dimension of the truncated space of modes available to us. If, at a given point in parameter space, the diagonalization of Eq. (19) with respect to fluctuations of order less than $N_{\rm max}$ yields at least one eigenvalue with a positive real component, it is thus sufficient to claim that the condensate is dynamically unstable up to linear order in the fluctuations.

We limit our analysis to the regions of parameter space explored in Figs. 1 and 4. As several modes might be unstable at a given point in parameter space, we merely work with the eigenvalue with the largest positive, real component, denoted by λ_0. Figure 5 plots $\lambda_0^{1/4}$ as a function of both $\epsilon_{\rm dd}$ and Ω, with the inset demonstrating how λ_0 behaves for the parameter space explored in the DGPE simulation via a cross section at fixed $\Omega = 3\omega_\perp$.

As $\epsilon_{\rm dd} \to 1$, more regions of parameter space become dynamically unstable to collective modes of polynomial order less than 14. In addition, the region that remains stable against these modes becomes smaller for larger Ω. The inset shows that for all nonzero $\epsilon_{\rm dd}$ (with $\Omega = 3\omega_\perp$ and $\gamma = 1$) the corresponding TF stationary solutions suffer dynamical instabilities, with the corresponding values of λ_0 growing as $\epsilon_{\rm dd} \to 1$. We also note that the amplitude of a mode corresponding to a real, positive eigenvalue λ_0, increases with an associated exponential timescale of $\Omega/(2\pi\lambda_0)$ rotation cycles. For $\epsilon_{\rm dd} = 0.1$, we find that $\lambda_0 \approx 0.05$, suggesting that the exponential timescale for amplitude growth is approximately 10 rotation cycles. For current experimental scenarios involving strongly dipolar species such as ^{164}Dy, a Feshbach resonance is generally utilized to tune $\epsilon_{\rm dd}$ to be slightly lower than 1

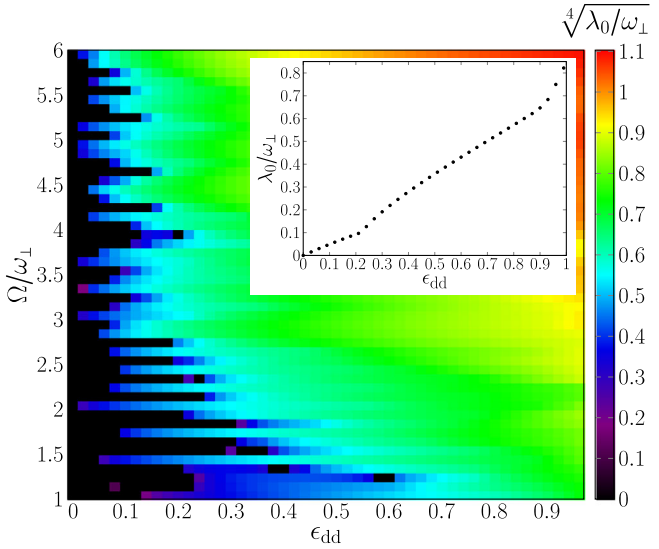

FIG. 5. Dynamical instability of the TF stationary states: $\sqrt[4]{\lambda_0}$ as a function of Ω and $\epsilon_{\rm dd}$ with $\gamma = 1$ and $N_{\rm max} = 13$. The prevalence of real, positive eigenvalues for $\epsilon_{\rm dd} > 0$ indicates the existence of a dynamical instability. Note that black corresponds to $\sqrt[4]{\lambda_0} = 0$. The inset takes a cross section at $\Omega = 3\omega_\perp$, corresponding to Figs. 3 and 4, and plots λ_0, showing that $\lambda_0 > 0 \ \forall \ \epsilon_{\rm dd} > 0$.

[4,6]. Figure 5 shows that for $\Omega/\omega_\perp = 6$ the dynamical instability manifests itself over a timescale of $1/\omega_\perp$ in a cylindrically symmetric trap. Decreasing Ω increases the timescale for manifestation of the instability.

Our method does not allow for direct modeling of the experimental report of rotationally tuned dipolar BECs by Tang *et al.* [30], since the relevant trap is not cylindrically symmetric. This would preclude the existence of stationary states in the rotating frame, which form the basis of our analysis. However, our formalism does describe a dipolar BEC in a cylindrically symmetric harmonic trap, with the radial trapping frequency matching the average x-y trapping frequency of that experiment. Therefore, we expect that accounting for the trapping ellipticity in the x-y plane would amount to a correction to the results obtained via our formalism. In this approximation, the timescale of the experiment is of the order of the typical timescale that we predict for the onset of the instability which, consequently, may not have fully manifested itself during the experimental observations. Nevertheless, the enhanced dissipation observed in the experiment may be linked to the onset of this instability and thus warrants further study. We also note that the considerable deviation from the theoretically predicted TF aspect ratio in the time-of-flight measurement for $\varphi = \pi/2$, the angle explored in our study, may be due to the presence of the instability.

In this Letter, we have examined the rotational tuning of harmonically trapped dipolar BECs, explicitly accounting for the rotation of the dipole polarization. This is performed by a semianalytical formalism for obtaining the TF stationary states of a dipolar BEC, validated through dGPE simulations. In the high-rotation frequency limit, the solutions converge to those of a dipolar BEC with a static time-averaged DDI potential, as previously predicted. Crucially, however, these solutions are dynamically unstable, with collective oscillations growing exponentially from perturbations. This prevents the formation of a stable long-lived rotationally tuned BEC. Our findings are of importance to the large body of theoretical work which has considered the rotationally tuned regime by assuming the robustness of the gas with the time-averaged DDI. They also suggest that experiments seeking to realize rotational tuning states must be carefully designed to avoid the seeding of instabilities and further DGPE studies should be carried out where the TF regime is not applicable. Finally, the TF formalism presented in this Letter may be generalized to account for an alignment of the dipoles at an arbitrary angle, φ, to the rotation axis.

S. B. P. is supported by an Australian Government Research Training Program Scholarship and by the University of Melbourne. A. M. M. would like to thank the Institute of Advanced Study (Durham University, UK) for hosting him during the initial stages of developing this collaborative research project and the Australian Research Council (Grant No. LE180100142) for support. T. B. and N. G. P. thank the Engineering and Physical Sciences Research Council of the UK (Grant No. EP/M005127/1) for support.

[1] A. Griesmaier, J. Werner, S. Hensler, J. Stuhler, and T. Pfau, Phys. Rev. Lett. **94**, 160401 (2005).
[2] Q. Beaufils, R. Chicireanu, T. Zanon, B. Laburthe-Tolra, E. Maréchal, L. Vernac, J. C. Keller, and O. Gorceix, Phys. Rev. A **77**, 061601(R) (2008).
[3] B. Pasquiou, G. Bismut, E. Maréchal, P. Pedri, L. Vernac, O. Gorceix, and B. Laburthe-Tolra, Phys. Rev. Lett. **106**, 015301 (2011).
[4] M. Lu, N. Q. Burdick, S. H. Youn, and B. L. Lev, Phys. Rev. Lett. **107**, 190401 (2011).
[5] K. Aikawa, A. Frisch, M. Mark, S. Baier, A. Rietzler, R. Grimm, and F. Ferlaino, Phys. Rev. Lett. **108**, 210401 (2012).
[6] H. Kadau, M. Schmitt, M. Wenzel, C. Wink, T. Maier, I. Ferrier-Barbut, and T. Pfau, Nature (London) **530**, 194 (2016).
[7] M. A. Baranov, Phys. Rep. **464**, 71 (2008).
[8] T. Lahaye, C. Menotti, L. Santos, M. Lewenstein, and T. Pfau, Rep. Prog. Phys. **72**, 126401 (2009).
[9] L. D. Carr, D. DeMille, and R. V. Krems, and J. Ye, New J. Phys. **11**, 055049 (2009).
[10] M. A. Baranov, M. Dalmonte, G. Pupillo, and P. Zoller, Chem. Rev. **112**, 5012 (2012).
[11] A. M. Martin, N. G. Marchant, D. H. J. O'Dell, and N. G. Parker, J. Phys.: Condens. Matter **29**, 103004 (2017).
[12] T. Lahaye, T. Koch, B. Fröhlich, M. Fattori, J. Metz, A. Griesmaier, S. Giovanazzi, and T. Pfau, Nature (London) **448**, 672 (2007).
[13] T. Lahaye, J. Metz, B. Fröhlich, T. Koch, M. Meister, A. Griesmaier, T. Pfau, H. Saito, Y. Kawaguchi, and M. Ueda, Phys. Rev. Lett. **101**, 080401 (2008).
[14] T. Koch, T. Lahaye, J. Metz, B. Fröhlich, A. Griesmaier, and T. Pfau, Nat. Phys. **4**, 218 (2008).
[15] M. Wenzel, F. Böttcher, J.-N. Schmidt, M. Eisenmann, T. Langen, T. Pfau, and I. Ferrier-Barbut,Phys. Rev. Lett. **121**, 030401 (2018).
[16] Y. Li, Y. Liu, Z. Fan, W. Pang, S. Fu, and B. A. Malomed, Phys. Rev. A **95**, 063613 (2017).
[17] L. Santos, G. V. Shlyapnikov, and M. Lewenstein, Phys. Rev. Lett. **90**, 250403 (2003).
[18] S. Ronen, D. C. E. Bortolotti, and J. L. Bohn, Phys. Rev. Lett. **98**, 030406 (2007).
[19] L. Chomaz, R. M. W. Bijnen, D. Petter, G. Faraoni, S. Baier, J. H. Becher, M. J. Mark, F. Wächtler, L. Santos, and F. Ferlaino, Nat. Phys. **14**, 442 (2018).
[20] M. Schmitt, M. Wenzel, F. Böttcher, I. Ferrier-Barbut, and T. Pfau, Nature (London) **539**, 259 (2016).
[21] I. Ferrier-Barbut, H. Kadau, M. Schmitt, M. Wenzel, and T. Pfau, Phys. Rev. Lett. **116**, 215301 (2016).
[22] L. Chomaz, S. Baier, D. Petter, M. J. Mark, F. Wächtler, L. Santos, and F. Ferlaino, Phys. Rev. X **6**, 041039 (2016).
[23] S. Giovanazzi, A. Görlitz, and T. Pfau, Phys. Rev. Lett. **89**, 130401 (2002).

[24] T. Bland, M. J. Edmonds, N. P. Proukakis, A. M. Martin, D. H. J. O'Dell, and N. G. Parker, Phys. Rev. A **92**, 063601 (2015).
[25] R. Nath, P. Pedri, and L. Santos, Phys. Rev. Lett. **101**, 210402 (2008).
[26] P. Pedri and L. Santos,Phys. Rev. Lett. **95**, 200404 (2005).
[27] M. J. Edmonds, T. Bland, R. Doran, and N. G. Parker, New J. Phys. **19**, 023019 (2017).
[28] T. Bland, G. W. Stagg, L. Galantucci, A. W. Baggaley, and N. G. Parker, Phys. Rev. Lett. **121**, 174501 (2018).
[29] M. Klawunn, R. Nath, P. Pedri, and L. Santos, Phys. Rev. Lett. **100**, 240403 (2008).
[30] Y. Tang, W. Kao, K.-Y. Li, and B. L. Lev, Phys. Rev. Lett. **120**, 230401 (2018).
[31] A. Recati, F. Zambelli, and S. Stringari, Phys. Rev. Lett. **86**, 377 (2001).
[32] S. Sinha and Y. Castin, Phys. Rev. Lett. **87**, 190402 (2001).
[33] N. G. Parker, R. M. W. van Bijnen, and A. M. Martin, Phys. Rev. A **73**, 061603(R) (2006).
[34] K. W. Madison, F. Chevy, W. Wohlleben, and J. Dalibard, Phys. Rev. Lett. **84**, 806 (2000).
[35] E. Hodby, G. Hechenblaikner, S. A. Hopkins, O. M. Maragò, and C. J. Foot, Phys. Rev. Lett. **88**, 010405 (2001).
[36] L. Santos, G. V. Shlyapnikov, P. Zoller, and M. Lewenstein, Phys. Rev. Lett. **85**, 1791 (2000).
[37] S. Yi and L. You, Phys. Rev. A **63**, 053607 (2001).
[38] N. G. Parker and D. H. J. O'Dell, Phys. Rev. A **78**, 041601(R) (2008).
[39] See Supplemental Material at http://link.aps.org/supplemental/10.1103/PhysRevLett.122.050401 for the derivation of the TF stationary solutions, details of numerical simulations, and the explicit expression for the operator $\mathcal{L}$, which includes Refs. [31,32,38,40–47].
[40] R. M. W. van Bijnen, A. J. Dow, D. H. J. O'Dell, N. G. Parker, and A. M. Martin, Phys. Rev. A **80**, 033617 (2009).
[41] D. H. J. O'Dell, S. Giovanazzi, and C. Eberlein, Phys. Rev. Lett. **92**, 250401 (2004).
[42] C. Eberlein, S. Giovanazzi, and D. H. J. O'Dell, Phys. Rev. A **71**, 033618 (2005).
[43] W. Bao and Y. Cai, Kinet. Relat. Models **6**, 1 (2013).
[44] R. M. W. van Bijnen, N. G. Parker, S. J. J. M. F. Kokkelmans, A. M. Martin, and D. H. J. O'Dell, Phys. Rev. A **82**, 033612 (2010).
[45] I. Sapina, T. Dahm, and N. Schopohl, Phys. Rev. A **82**, 053620 (2010).
[46] W. Bao and H. Wang, J. Comput. Phys. **217**, 612 (2006).
[47] S. Ronen, D. C. E. Bortolotti, D. Blume, and J. L. Bohn, Phys. Rev. A **74**, 033611 (2006).
[48] K. W. Madison, F. Chevy, V. Bretin, and J. Dalibard, Phys. Rev. Lett. **86**, 4443 (2001).
[49] R. M. W. van Bijnen, D. H. J. O'Dell, N. G. Parker, and A. M. Martin, Phys. Rev. Lett. **98**, 150401 (2007).
[50] L. Pitaevskii and S. Stringari, *Bose-Einstein Condensation*, International Series of Monographs on Physics (Clarendon, Oxford, 2003), p. 116.
[51] G. Bismut, B. Pasquiou, E. Maréchal, P. Pedri, L. Vernac, O. Gorceix, and B. Laburthe-Tolra, Phys. Rev. Lett. **105**, 040404 (2010).
[52] S. Stringari, Phys. Rev. Lett. **77**, 2360 (1996).

Author/s:
Prasad, SB; Bland, T; Mulkerin, BC; Parker, NG; Martin, AM

Title:
Instability of Rotationally Tuned Dipolar Bose-Einstein Condensates

Date:
2019-02-06

Citation:
Prasad, S. B., Bland, T., Mulkerin, B. C., Parker, N. G. & Martin, A. M. (2019). Instability of Rotationally Tuned Dipolar Bose-Einstein Condensates. Physical Review Letters, 122 (5), https://doi.org/10.1103/PhysRevLett.122.050401.